

Chapter 5

The electron liquid *(Last version: 28 September 2011)*

Contents

5.1	The jellium model	340
5.2	The random-phase approximation (RPA)	341
5.2.1	Dielectric function and density-density response function .	341
5.2.2	Mean-field character of the RPA	343
5.2.3	The RPA in the functional integral formalism	344
5.3	Physical properties of the RPA	347
5.3.1	The Lindhard function	347
5.3.2	Density fluctuation spectrum	350
5.3.3	Screening	352
5.3.4	Ground state energy and compressibility	354
5.4	One-particle properties	357
5.4.1	Hartree-Fock theory	357
5.4.2	RPA self-energy	359
5.5	Beyond the RPA	361

The aim of this chapter is twofold. On the one hand, we wish to give a short (and incomplete) description of the electron liquid. The analysis is based on the jellium model where the electrons interact *via* the Coulomb interaction and the neutrality of the system is maintained by a uniform background of positive charge with infinite inertia. We discuss the results obtained within the random-phase approximation (RPA): plasmon mode, screening, Fermi-liquid behavior, etc. In this respect, this chapter is complementary to our discussion of the neutral Fermi liquid (chapter 4) as well as the general considerations of section 3.4. On the other hand, the electron liquid provides an opportunity to introduce standard many-body approaches (RPA, (time-dependent) Hartree-Fock theory) that come up in different contexts, and discuss in particular how they are formulated within diagrammatic or functional integral techniques. We deal only with a three-dimensional electron liquid at zero temperature. More specialized references on the subject are given in the bibliography at the end of the chapter.

5.1 The jellium model

In the jellium model, one assumes that the global neutrality of the system is maintained by the presence of a uniform background of positive charge. This can be seen as a first approximation to a metallic system. In a real crystal the positive charge (ions) is not uniform and can also have its own dynamics (lattice vibrations).

The Hamiltonian reads $\hat{H} = \hat{H}_0 + \hat{H}_{\text{int}} + \hat{H}_{e-b} + \hat{H}_{b-b}$, where

$$\begin{aligned}\hat{H}_0 &= \sum_{i=1}^N \frac{\hat{p}_i^2}{2m}, \\ \hat{H}_{\text{int}} &= \frac{1}{2} \sum_{\substack{i,j=1 \\ i \neq j}}^N \frac{e^2}{4\pi\epsilon_0 |\hat{\mathbf{r}}_i - \hat{\mathbf{r}}_j|},\end{aligned}\tag{5.1}$$

are the kinetic and interaction Hamiltonians of the electrons. In second-quantized form, one obtains

$$\begin{aligned}\hat{H}_0 &= \sum_{\mathbf{k},\sigma} \xi_{\mathbf{k}} \hat{\psi}_{\sigma}^{\dagger}(\mathbf{k}) \hat{\psi}_{\sigma}(\mathbf{k}), \\ \hat{H}_{\text{int}} &= \frac{1}{2V} \sum_{\substack{\mathbf{k},\mathbf{k}',\mathbf{q} \\ \sigma,\sigma'}} v(\mathbf{q}) \hat{\psi}_{\sigma}^{\dagger}(\mathbf{k} + \mathbf{q}) \hat{\psi}_{\sigma'}^{\dagger}(\mathbf{k}' - \mathbf{q}) \hat{\psi}_{\sigma'}(\mathbf{k}') \hat{\psi}_{\sigma}(\mathbf{k}) \\ &= \frac{1}{2} \sum_{\mathbf{q}} v(\mathbf{q}) \left[\hat{n}(-\mathbf{q}) \hat{n}(\mathbf{q}) - \frac{\hat{N}}{V} \right],\end{aligned}\tag{5.2}$$

where

$$\hat{n}(\mathbf{q}) = \frac{1}{\sqrt{V}} \int d^3r e^{-i\mathbf{q}\cdot\mathbf{r}} \hat{n}(\mathbf{r}) = \frac{1}{\sqrt{V}} \sum_{\mathbf{k},\sigma} \hat{\psi}_{\sigma}^{\dagger}(\mathbf{k}) \hat{\psi}_{\sigma}(\mathbf{k} + \mathbf{q})\tag{5.3}$$

is the Fourier transform of the density operator $\hat{n}(\mathbf{r}) = \sum_{\sigma} \hat{\psi}_{\sigma}^{\dagger}(\mathbf{r}) \hat{\psi}_{\sigma}(\mathbf{r})$. $v(\mathbf{q}) = e^2/\epsilon_0 \mathbf{q}^2$ is the Fourier transform of the Coulomb potential $e^2/4\pi\epsilon_0 |\mathbf{r}|$. We now use the grand canonical ensemble and include the term $-\mu \hat{N}$ into the Hamiltonian \hat{H}_0 ($\xi_{\mathbf{k}} = \mathbf{k}^2/2m - \mu$). The background of positive charge gives rise to the two additional terms

$$\begin{aligned}\hat{H}_{e-b} &= -e^2 \int d^3r d^3r' \frac{n \hat{n}(\mathbf{r})}{4\pi\epsilon_0 |\mathbf{r} - \mathbf{r}'|} = -v(0) n \hat{N}, \\ \hat{H}_{b-b} &= \frac{e^2}{2} \int d^3r d^3r' \frac{n^2}{4\pi\epsilon_0 |\mathbf{r} - \mathbf{r}'|} = \frac{1}{2} n^2 V v(0),\end{aligned}\tag{5.4}$$

where $v(0) \equiv v(\mathbf{q} = 0)$. \hat{H}_{b-b} gives the electrostatic energy of the uniform background of charge density $-en$ ($n = N/V$ is the electron density), and \hat{H}_{e-b} the interaction energy between the positive background and the electrons.

Because of the long-range nature of the Coulomb interaction, the integrals appearing in (5.4) are not convergent and $v(0)$ is not defined. Since the system is neutral, the various infinities should cancel and the energy of the system be finite. To deal

with this difficulty, one regularizes the Coulomb interaction by choosing

$$v(\mathbf{r}) = \frac{e^2}{4\pi\epsilon_0} \frac{e^{-\kappa|\mathbf{r}|}}{|\mathbf{r}|}, \quad \text{i.e.} \quad v(\mathbf{q}) = \frac{e^2}{\epsilon_0(\mathbf{q}^2 + \kappa^2)}. \quad (5.5)$$

All terms in (5.4) are now well defined. Physical quantities are obtained by taking first the thermodynamic limit $V \rightarrow \infty$ and then $\kappa \rightarrow 0$. This procedure can be justified *a posteriori* by noting that the final results are independent of κ .

The part of the Hamiltonian \hat{H} involving $v(0) = v(\mathbf{q} = 0)$ reads

$$\frac{1}{2V}v(0)(\hat{N}^2 - \hat{N}) - v(0)n\hat{N} + \frac{1}{2}Vv(0)n^2 \simeq -\frac{1}{2}v(0)n, \quad (5.6)$$

since the fluctuations of the operator \hat{N} becomes negligible in the thermodynamic limit.¹ The energy $\langle \hat{H} \rangle$ being an extensive quantity, the part involving $v(0)$ is of relative order

$$\frac{v(0)n}{V} = \frac{ne^2}{V\epsilon_0\kappa^2} \quad (5.7)$$

and vanishes in the thermodynamic limit ($V \rightarrow \infty$ with κ fixed). Thus we see that $\hat{H}_{e-b} + \hat{H}_{b-b}$ cancel the $\mathbf{q} = 0$ term in \hat{H}_{int} . The Hamiltonian in the jellium model can therefore be written as $\hat{H}_0 + \hat{H}_{\text{int}}$ without the $\mathbf{q} = 0$ term in \hat{H}_{int} . It is convenient to define $v(\mathbf{q})$ as $(1 - \delta_{\mathbf{q},0})e^2/\epsilon_0\mathbf{q}^2$ so that $v(0) = 0$.

5.2 The random-phase approximation (RPA)

The RPA is one of the simplest approximations to the density-density response function and the dynamic longitudinal dielectric function of the electron liquid. In this section we derive the RPA from several points of view. In particular we shall see that the RPA arises very naturally in the functional integral formalism.

5.2.1 Dielectric function and density-density response function

In section 3.4.1 we have shown that the longitudinal dielectric function $\epsilon_{\parallel}(q)$ is related to the density-density response function $\chi_{nn}(q)$,

$$\frac{1}{\epsilon_{\parallel}(q)} = 1 - v(\mathbf{q})\chi_{nn}(q) \quad \text{or} \quad \epsilon_{\parallel}(q) = 1 + v(\mathbf{q})\Pi_{nn}(q), \quad (5.8)$$

where $\Pi_{nn}(q)$ is the ‘‘irreducible’’ part of the $\chi_{nn}(q)$, i.e. the part that cannot be split into two disconnected pieces by cutting a single Coulomb line $v(\mathbf{q})$. The general properties of χ_{nn} and ϵ_{\parallel} were discussed in section 3.4.1. In particular, we have shown that $\epsilon_{\parallel}^R(\mathbf{q}, \omega)$ satisfies a number of sum rules (table 5.1). These sum rules, together with the fact that the particle-hole pair excitations do not contribute to the spectral function $\Im[1/\epsilon_{\parallel}^R(\mathbf{q}, \omega)]$ for $\mathbf{q} \rightarrow 0$, imply that the electron liquid possesses a (collective) plasmon mode with energy $\omega_p = (ne^2/\epsilon_0 m)^{1/2}$ in the long wavelength limit.

¹ $\lim_{V \rightarrow \infty} \frac{\sqrt{\langle \hat{N}^2 \rangle - \langle \hat{N} \rangle^2}}{\langle \hat{N} \rangle} \sim \frac{1}{\sqrt{\langle \hat{N} \rangle}}$.

f -sum rule	$\int_{-\infty}^{\infty} \frac{d\omega}{\pi} \omega \Im \left[\frac{1}{\epsilon_{\parallel}^R(\mathbf{q}, \omega)} \right] = -\omega_p^2$
perfect-screening sum rule	$\lim_{\mathbf{q} \rightarrow 0} \int_{-\infty}^{\infty} \frac{d\omega}{\pi} \frac{1}{\omega} \Im \left[\frac{1}{\epsilon_{\parallel}^R(\mathbf{q}, \omega)} \right] = -1$
longitudinal conductivity sum rule	$\int_{-\infty}^{\infty} \frac{d\omega}{\pi} \omega \Im [\epsilon_{\parallel}^R(\mathbf{q}, \omega)] = \omega_p^2$
compressibility sum rule	$\lim_{\mathbf{q} \rightarrow 0} \int_{-\infty}^{\infty} \frac{d\omega}{\pi} \frac{1}{\omega} \Im [\epsilon_{\parallel}^R(\mathbf{q}, \omega)] = \frac{e^2 n^2 \kappa}{\epsilon_0 \mathbf{q}^2}$

Table 5.1: Sum rules satisfied by the longitudinal dielectric function $\epsilon_{\parallel}^R(\mathbf{q}, \omega)$ (see Sec. 3.4.1). κ denotes the compressibility and ω_p the plasma frequency.

An explicit expression of $\epsilon_{\parallel}(q)$ and $\chi_{nn}(q)$ requires to compute, at least approximately, the irreducible part $\Pi_{nn}(q)$.² In the following, we consider the zeroth-order approximation – known as the random phase approximation – where Π_{nn} is identified with the non-interacting susceptibility (Fig. 5.1),

$$\Pi_{nn}^{\text{RPA}}(q) = \chi_{nn}^0(q) = -\frac{2}{\beta V} \sum_k G_0(k) G_0(k+q). \quad (5.9)$$

This gives

$$\chi_{nn}^{\text{RPA}}(q) = \frac{\chi_{nn}^0(q)}{1 + v(\mathbf{q})\chi_{nn}^0(q)} \quad \text{and} \quad \epsilon_{\parallel}^{\text{RPA}}(q) = 1 + v(\mathbf{q})\chi_{nn}^0(q). \quad (5.10)$$

The density-density response function χ_{nn}^{RPA} can be represented by the sum of bubble diagrams shown in figure 5.2.

To estimate the domain of validity of a perturbative treatment of the Coulomb interaction, we consider the ratio

$$\frac{\text{Potential energy}}{\text{Kinetic energy}} \sim \frac{e^2}{\epsilon_0 n^{-1/3}} \sim \frac{e^2 m}{\epsilon_0 k_F} \sim \frac{1}{n^{1/3} a_0}, \quad (5.11)$$

where $a_0 = \hbar^2 \epsilon_0 / \pi m e^2$ is the Bohr radius. It is customary to write the volume per particle as

$$\frac{1}{n} = \frac{3\pi^2}{k_F^3} = \frac{4}{3} \pi (r_s a_0)^3 \quad (5.12)$$

so that

$$\frac{\text{Potential energy}}{\text{Kinetic energy}} \sim r_s. \quad (5.13)$$

²Note that Π_{nn} is the right quantity to consider in order to obtain satisfying expressions for χ_{nn} and ϵ_{\parallel} . Any approximate Π_{nn} will give a result for χ_{nn} and ϵ_{\parallel} to infinite order in the Coulomb interaction. By contrast, a finite order approximation to χ_{nn} is likely to violate basic properties such as causality. This is the case for instance if one retains only the first two diagrams in figure 5.2. Note that a similar observation was made when discussing the one-particle Green function G (Sec. 3.5): the self-energy Σ (and not G) is the right quantity to consider in perturbation theory.

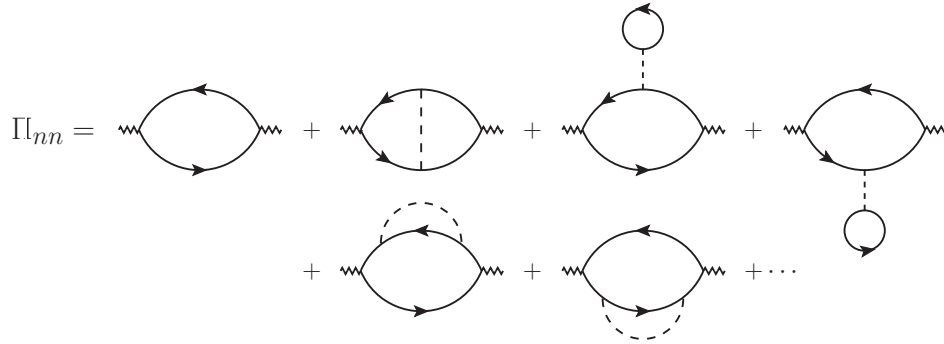


Figure 5.1: Lowest-order contributions to Π_{nn} . The RPA retains only the zeroth-order term.

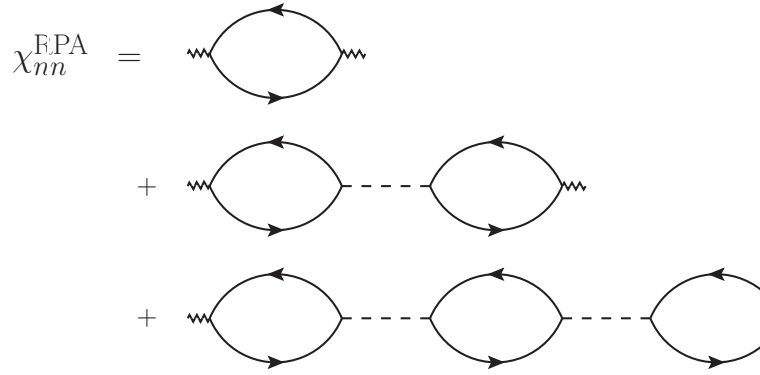


Figure 5.2: Diagrammatic representation of the density-density response function χ_{nn} in the RPA.

Thus the RPA is expected to be justified at high density when $r_s \ll 1$. Since typical metals correspond to a range $r_s \sim 2 - 5$, the RPA results have limited applicability even for conventional metals. In section 5.5 we briefly discuss how one can go beyond the RPA. In the opposite limit $r_s \gg 1$, the electrons are expected to localize and form a Wigner crystal since at very low density the zero-point kinetic energy associated with localizing the electrons eventually becomes negligible in comparison with the electrostatic energy of a classical lattice.

5.2.2 Mean-field character of the RPA

To see the mean-field character of the RPA, let us rederive it within an elementary approach. We consider the system in the presence of an external potential

$$\phi_{\text{ext}}(\mathbf{r}, t) = \frac{1}{\sqrt{V}} \sum_{\mathbf{q}} \phi_{\text{ext}}(\mathbf{q}, \omega) e^{i[\mathbf{q} \cdot \mathbf{r} - (\omega + i\eta)t]} + \text{c.c.} \quad (5.14)$$

($\eta \rightarrow 0^+$). Keeping only the part that oscillates with $e^{i[\mathbf{q}\cdot\mathbf{r}-(\omega+i\eta)t]}$ (we are interested only in the linear response to ϕ_{ext}), the Hamiltonian reads

$$\hat{H} = \hat{H}_0 + \frac{1}{2} \sum_{\mathbf{q}} v(\mathbf{q}) \left[\hat{n}(-\mathbf{q})\hat{n}(\mathbf{q}) - \frac{\hat{N}}{V} \right] + \sum_{\mathbf{q}} \phi_{\text{ext}}(\mathbf{q}, \omega) e^{-i(\omega+i\eta)t} \hat{n}(-\mathbf{q}). \quad (5.15)$$

The term \hat{N}/V can be ignored since it does not play any role in the following argument. In a mean-field approximation, the interacting Hamiltonian \hat{H}_{int} is linearized with respect to the fluctuations $\delta\hat{n}(\mathbf{q}) = \hat{n}(\mathbf{q}) - \langle\hat{n}(\mathbf{q})\rangle$ of the density operator,

$$\begin{aligned} \hat{n}(-\mathbf{q})\hat{n}(\mathbf{q}) &= [\delta\hat{n}(-\mathbf{q}) + \langle\hat{n}(-\mathbf{q})\rangle][\delta\hat{n}(\mathbf{q}) + \langle\hat{n}(\mathbf{q})\rangle] \\ &= \delta\hat{n}(-\mathbf{q})\langle\hat{n}(\mathbf{q})\rangle + \langle\hat{n}(-\mathbf{q})\rangle\delta\hat{n}(\mathbf{q}) + \langle\hat{n}(-\mathbf{q})\rangle\langle\hat{n}(\mathbf{q})\rangle + \mathcal{O}(\delta\hat{n}^2) \\ &= \hat{n}(-\mathbf{q})\langle\hat{n}(\mathbf{q})\rangle + \langle\hat{n}(-\mathbf{q})\rangle\hat{n}(\mathbf{q}) - \langle\hat{n}(-\mathbf{q})\rangle\langle\hat{n}(\mathbf{q})\rangle + \mathcal{O}(\delta\hat{n}^2), \end{aligned} \quad (5.16)$$

so that

$$\hat{H}_{\text{MF}} = \hat{H}_0 + \sum_{\mathbf{q}} [\phi_{\text{ext}}(\mathbf{q}, \omega) e^{-i(\omega+i\eta)t} + v(\mathbf{q})\langle\hat{n}(\mathbf{q})\rangle] \hat{n}(-\mathbf{q}) \quad (5.17)$$

up to an irrelevant constant. We are therefore left with a system of free electrons subject to the effective potential

$$\phi_{\text{eff}}(\mathbf{q}, t) = \phi_{\text{ext}}(\mathbf{q}, \omega) e^{-i(\omega+i\eta)t} + v(\mathbf{q})\langle\hat{n}(\mathbf{q})\rangle. \quad (5.18)$$

The linear response to a scalar potential is given by the density-density response function (Sec. 3.3). We thus have

$$\begin{aligned} \langle\hat{n}(\mathbf{q})\rangle &= -\chi_{nn}^{0R}(\mathbf{q}, \omega) \phi_{\text{eff}}(\mathbf{q}, \omega) e^{-i(\omega+i\eta)t} \\ &= -\chi_{nn}^R(\mathbf{q}, \omega) \phi_{\text{ext}}(\mathbf{q}, \omega) e^{-i(\omega+i\eta)t}, \end{aligned} \quad (5.19)$$

and therefore

$$\chi_{nn}^R(\mathbf{q}, \omega) = \frac{\chi_{nn}^{0R}(\mathbf{q}, \omega)}{1 + v(\mathbf{q})\chi_{nn}^{0R}(\mathbf{q}, \omega)}, \quad (5.20)$$

which is the RPA result.

5.2.3 The RPA in the functional integral formalism

Hubbard-Stratonovich transformation

We consider the action $S = S_0 + S_{\text{int}} + S_J$ in the presence of external sources that couple to the density,

$$\begin{aligned} S_{\text{int}} &= \frac{1}{2\beta V} \sum_{\substack{k, k', q \\ \sigma, \sigma'}} v(\mathbf{q}) \psi_{\sigma}^*(k+q) \psi_{\sigma'}^*(k'-q) \psi_{\sigma'}(k') \psi_{\sigma}(k) \\ &= \frac{1}{2} \sum_q v(\mathbf{q}) n(-q) n(q), \\ S_J &= - \sum_q J(-q) n(q), \end{aligned} \quad (5.21)$$

where

$$n(q) = \frac{1}{\sqrt{\beta V}} \sum_{k,\sigma} \psi_\sigma^*(k) \psi_\sigma(k+q). \quad (5.22)$$

We rewrite S_{int} by means of a Gaussian functional integral over an auxiliary real bosonic field $\phi(x)$,

$$\exp\{-S_{\text{int}}\} = \mathcal{N} \int \mathcal{D}[\phi] \exp\left\{-\frac{1}{2} \sum_q \phi(-q) v(\mathbf{q})^{-1} \phi(q) + i \sum_q \phi(-q) n(q)\right\}. \quad (5.23)$$

The normalization constant $\mathcal{N} = \det(v^{-1/2})$ will be ignored in the following. This kind of transformation – known as a Hubbard-Stratonovich transformation – will be used repeatedly in this book.³ It transforms a system of interacting particles into a system of “free” particles interacting with a bosonic field. The action now reads

$$S[\psi^*, \psi, \phi] = S_0[\psi^*, \psi] + \frac{1}{2} \sum_q \left\{ \phi(-q) v(\mathbf{q})^{-1} \phi(q) - 2[i\phi(-q) + J(-q)]n(q) \right\}, \quad (5.24)$$

and the partition function involves a functional integral over both the fermionic field ψ and the bosonic field ϕ . Note that the Hubbard-Stratonovich field ϕ is nothing but the scalar potential of the electromagnetic field (Sec. 1.9.3).⁴ Its propagator can therefore be expressed in terms of the dielectric function,

$$D_{00}(q) = \langle \phi(q) \phi(-q) \rangle = \frac{v(\mathbf{q})}{\epsilon_{\parallel}(q)}. \quad (5.25)$$

Saddle-point approximation: Hartree theory

The Hubbard-Stratonovich transformation suggests various approximations to treat the electron-electron interactions (now encoded in the dynamics of the bosonic field ϕ). The simplest one amounts to performing a saddle-point (or mean-field) approximation for the functional integral over ϕ whereby

$$Z = \int \mathcal{D}[\psi^*, \psi, \phi] \exp\{-S[\psi^*, \psi, \phi]\} \rightarrow Z_{\text{MF}} = \int \mathcal{D}[\psi^*, \psi] \exp\{-S_{\text{MF}}[\psi^*, \psi]\}. \quad (5.26)$$

The mean field $\phi(q) = \sqrt{\beta V} \delta_{q,0} \phi_0$ (i.e. $\phi(x) = \phi_0$) is chosen static and uniform. For $J = 0$, the mean-field action reads

$$S_{\text{MF}}[\psi^*, \psi] = \frac{\beta V}{2} v(0)^{-1} \phi_0^2 - \sum_{k,\sigma} \psi_\sigma^*(k) (i\omega_n - \xi_{\mathbf{k}} + i\phi_0) \psi_\sigma(k). \quad (5.27)$$

The value of ϕ_0 is determined by requiring the thermodynamic potential to be minimum: $\partial\Omega_{\text{MF}}/\partial\phi_0 = 0$ or, equivalently, $\partial Z_{\text{MF}}/\partial\phi_0 = 0$. This gives

$$\int \mathcal{D}[\psi^*, \psi] \left[\beta V v(0)^{-1} \phi_0 - i \sum_{k,\sigma} \psi_\sigma^*(k) \psi_\sigma(k) \right] \exp\{-S_{\text{MF}}[\psi^*, \psi]\} = 0, \quad (5.28)$$

³See Sec. 6.3.3 for a discussion of the limitations of Hubbard-Stratonovich transformations.

⁴ ϕ differs from the scalar potential by a factor e (the electron charge). Recall also that $i\phi$ plays the role of the scalar potential in the imaginary time formalism.

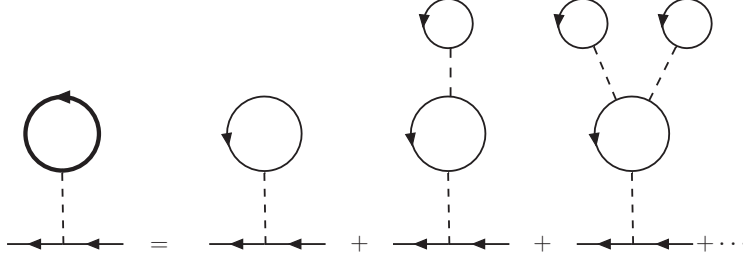


Figure 5.3: Hartree self-energy Σ_{H} . The thick solid line denotes the Green function $G = (G_0 - \Sigma_{\text{H}})^{-1}$.

i.e.

$$i\phi_0 = -v(0) \frac{1}{\beta V} \sum_{k,\sigma} \langle \psi_{\sigma}^*(k) \psi_{\sigma}(k) \rangle e^{i\omega_n \eta} = -v(0)n \quad (5.29)$$

(we have added the usual convergence factor). Note that ϕ_0 is purely imaginary, which ensures that the mean-field action is real.⁵ The result (5.29) has a simple interpretation in terms of Feynman diagrams. It corresponds to the first-order self-consistent self-energy shown in figure 5.3,

$$\Sigma_{\text{H}}(k) = v(0) \frac{1}{\beta V} \sum_{k,\sigma} G_{\sigma}(k) e^{i\omega_n \eta} = v(0)n. \quad (5.30)$$

In the jellium model, $v(0) = 0$ and the Hartree self-energy (5.30) vanishes ($\phi_0 = 0$). In short-range interaction models however, Σ_{H} is in general finite. Being independent of k , it merely renormalizes the chemical potential.

Gaussian fluctuations: RPA

To proceed beyond the saddle-point approximation, we derive the effective action of the bosonic field to second order in $\phi(x) - \phi_0 \equiv \phi(x)$. To do so, one has to integrate out the ψ field retaining only the second-order cumulant,⁶

$$\begin{aligned} Z[J] &= \int \mathcal{D}[\psi^*, \psi, \phi] \exp\left\{-S_0[\psi^*, \psi] \right. \\ &\quad \left. - \frac{1}{2} \sum_q [\phi(-q)v(\mathbf{q})^{-1}\phi(q) - 2[i\phi(-q) + J(-q)]n(q)]\right\} \\ &= Z_0 \int \mathcal{D}[\phi] \exp\{-S[\phi]\}, \end{aligned} \quad (5.31)$$

⁵Recall that mathematically there is nothing that prevents the saddle point ϕ_0 to be imaginary even though the auxiliary bosonic field $\phi(x)$ is real. One can deform the integration contour into the complex plane when looking for a saddle point.

⁶The first-order cumulant gives a trivial contribution $\sum_q [i\phi(-q) + J(-q)]\langle n(q) \rangle = J(q=0)\sqrt{\beta V}n$ to the action (the ϕ field has no $q=0$ component since $v(0) = 0$).

where

$$S[\phi] = \frac{1}{2} \sum_{\mathbf{q}} \left\{ \phi(-\mathbf{q}) v(\mathbf{q})^{-1} \phi(\mathbf{q}) - [i\phi(-\mathbf{q}) + J(-\mathbf{q})] \chi_{nn}^0(\mathbf{q}) [i\phi(\mathbf{q}) + J(\mathbf{q})] \right\}. \quad (5.32)$$

For $J = 0$, one obtains the propagator of the auxiliary field,

$$D_{00}(q) = \langle \phi(q) \phi(-q) \rangle = \frac{1}{v(\mathbf{q})^{-1} + \chi_{nn}^0(q)} = \frac{v(\mathbf{q})}{1 + v(\mathbf{q}) \chi_{nn}^0(q)}, \quad (5.33)$$

which reproduces the RPA result (5.10) for the longitudinal dielectric function (compare (5.25) and (5.33)). From the action (5.32), one can also obtain the partition function by integrating out the ϕ field,

$$Z[J] = Z_0 \exp \left\{ \frac{1}{2} \sum_{\mathbf{q}} J(-\mathbf{q}) \left[\chi_{nn}^0(q) - \frac{v(\mathbf{q}) [\chi_{nn}^0(q)]^2}{1 + v(\mathbf{q}) \chi_{nn}^0(q)} \right] J(\mathbf{q}) \right\}, \quad (5.34)$$

and deduce the density-density correlation function

$$\chi_{nn}(q) = \left. \frac{\delta^{(2)} \ln Z[J]}{\delta J(-q) \delta J(q)} \right|_{J=0} = \frac{\chi_{nn}^0(q)}{1 + v(\mathbf{q}) \chi_{nn}^0(q)}. \quad (5.35)$$

Thus we see that by taking into account the Gaussian fluctuations of ϕ about the saddle point ϕ_0 , we reproduce the RPA.

5.3 Physical properties of the RPA

In this section, we discuss some basic properties of the electron liquid in the RPA: density fluctuations spectrum and plasmon mode, screening, ground-state energy and compressibility. We begin with a calculation of the Lindhard function χ_{nn}^{0R} .

5.3.1 The Lindhard function

After summation over the Matsubara frequency in (5.9) and the analytic continuation $i\omega_\nu \rightarrow \omega + i\eta$,⁷ one obtains the retarded response function (or Lindhard function)

$$\chi_{nn}^{0R}(\mathbf{q}, \omega) = -\frac{2}{V} \sum_{\mathbf{k}} \frac{n_F(\xi_{\mathbf{k}}) - n_F(\xi_{\mathbf{k}+\mathbf{q}})}{\omega + i\eta + \xi_{\mathbf{k}} - \xi_{\mathbf{k}+\mathbf{q}}}. \quad (5.36)$$

An elementary change of variables gives

$$\chi_{nn}^{0R}(\mathbf{q}, \omega) = -\frac{2}{V} \sum_{\mathbf{k}} \frac{n_F(\xi_{\mathbf{k}})}{\omega + i\eta + \xi_{\mathbf{k}} - \xi_{\mathbf{k}+\mathbf{q}}} + (\omega + i\eta \rightarrow -\omega - i\eta), \quad (5.37)$$

⁷The Matsubara sum is done explicitly in Appendix 1.F.

with $n_F(\xi_{\mathbf{k}}) = \Theta(k_F - |\mathbf{k}|)$ at zero temperature. Introducing the dimensionless variables $x = |\mathbf{k}|/k_F$, $\tilde{q} = |\mathbf{q}|/k_F$ and $\tilde{\omega}^+ = (\omega + i\eta)/v_F|\mathbf{q}|$, we have

$$\begin{aligned} \int \frac{d^3k}{(2\pi)^3} \frac{\Theta(k_F - |\mathbf{k}|)}{\omega + i\eta + \xi_{\mathbf{k}} - \xi_{\mathbf{k}+\mathbf{q}}} &= \frac{1}{4\pi^2} \int_0^{k_F} k^2 dk \int_0^\pi d\theta \frac{\sin \theta}{\omega + i\eta - \frac{|\mathbf{k}||\mathbf{q}|}{m} \cos \theta - \frac{\mathbf{q}^2}{2m}} \\ &= \frac{mk_F^2}{4\pi^2|\mathbf{q}|} \int_0^1 dx x^2 \int_0^\pi \frac{\sin \theta}{\tilde{\omega}^+ - x \cos \theta - \frac{\tilde{q}}{2}} \\ &= \frac{N(0)}{2\tilde{q}} \int_0^1 dx x \ln \left(\frac{\tilde{\omega}^+ + x - \tilde{q}/2}{\tilde{\omega}^+ - x - \tilde{q}/2} \right) \\ &= \frac{N(0)}{2\tilde{q}} \left[a - \frac{a^2 - 1}{2} \ln \left(\frac{a + 1}{a - 1} \right) \right], \end{aligned} \quad (5.38)$$

where $a = \tilde{\omega}^+ - \tilde{q}/2$. $N(0) = mk_F/2\pi^2$ is the non-interacting density of states per spin at $\xi_{\mathbf{k}} = 0$. From (5.37) and (5.38), we finally obtain

$$\begin{aligned} \chi_{nn}^{0R}(\mathbf{q}, \omega) &= N(0) \left\{ 1 - \frac{1}{2\tilde{q}} \left[1 - \left(\tilde{\omega}^+ - \frac{\tilde{q}}{2} \right)^2 \right] \ln \left(\frac{\tilde{\omega}^+ + 1 - \tilde{q}/2}{\tilde{\omega}^+ - 1 - \tilde{q}/2} \right) \right. \\ &\quad \left. - \frac{1}{2\tilde{q}} \left[1 - \left(\tilde{\omega}^+ + \frac{\tilde{q}}{2} \right)^2 \right] \ln \left(\frac{\tilde{\omega}^+ - 1 + \tilde{q}/2}{\tilde{\omega}^+ + 1 + \tilde{q}/2} \right) \right\}. \end{aligned} \quad (5.39)$$

The real and imaginary parts of the Lindhard function read

$$\begin{aligned} \Re[\chi_{nn}^{0R}(\mathbf{q}, \omega)] &= N(0) \left\{ 1 - \frac{1}{2\tilde{q}} \left[1 - \left(\tilde{\omega} - \frac{\tilde{q}}{2} \right)^2 \right] \ln \left| \frac{\tilde{\omega} + 1 - \tilde{q}/2}{\tilde{\omega} - 1 - \tilde{q}/2} \right| \right. \\ &\quad \left. - \frac{1}{2\tilde{q}} \left[1 - \left(\tilde{\omega} + \frac{\tilde{q}}{2} \right)^2 \right] \ln \left| \frac{\tilde{\omega} - 1 + \tilde{q}/2}{\tilde{\omega} + 1 + \tilde{q}/2} \right| \right\} \end{aligned} \quad (5.40)$$

and

$$\begin{aligned} \Im[\chi_{nn}^{0R}(\mathbf{q}, \omega)] &= N(0) \frac{\pi}{2\tilde{q}} \left\{ \left[1 - \left(\tilde{\omega} - \frac{\tilde{q}}{2} \right)^2 \right] \Theta \left[1 - \left(\tilde{\omega} - \frac{\tilde{q}}{2} \right)^2 \right] \right. \\ &\quad \left. - \left[1 - \left(\tilde{\omega} + \frac{\tilde{q}}{2} \right)^2 \right] \Theta \left[1 - \left(\tilde{\omega} + \frac{\tilde{q}}{2} \right)^2 \right] \right\}, \end{aligned} \quad (5.41)$$

where $\tilde{\omega} = \omega/v_F|\mathbf{q}|$.

For $\omega = 0$, the Lindhard function is real and given by

$$\chi_{nn}^{0R}(\mathbf{q}, 0) = N(0) \left[1 - \frac{1}{\tilde{q}} \left(1 - \frac{\tilde{q}^2}{4} \right) \ln \left| \frac{\tilde{q} - 2}{\tilde{q} + 2} \right| \right]. \quad (5.42)$$

In section 5.3.3 we shall see the non-analyticity at $\tilde{q} = 2$ has important consequences. For $|\mathbf{q}| \rightarrow 0$ and $\tilde{\omega} = \omega/v_F|\mathbf{q}|$ fixed, χ_{nn}^{0R} takes the form

$$\lim_{\substack{|\mathbf{q}| \rightarrow 0 \\ \tilde{\omega} \text{ fixed}}} \chi_{nn}^{0R}(\mathbf{q}, \omega) = 2N(0) \left[1 - \frac{\tilde{\omega}^+}{2} \left(\frac{\tilde{\omega}^+ + 1}{\tilde{\omega}^+ - 1} \right) \right], \quad (5.43)$$

a result previously obtained in Fermi-liquid theory (Sec. 4.3.4).

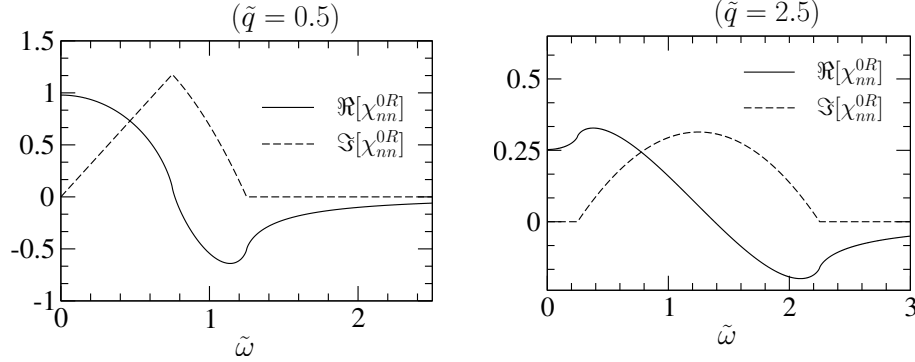


Figure 5.4: Real and imaginary parts of the Lindhard function $\chi_{nn}^{0R}(\mathbf{q}, \omega)/2N(0)$ for $|\mathbf{q}| = 0.5k_F$ and $|\mathbf{q}| = 2.5k_F$.

Spectral function $\chi_{nn}^{0''}(\mathbf{q}, \omega) = \Im[\chi_{nn}^{0R}(\mathbf{q}, \omega)]$

For $\tilde{q} \leq 2$, the imaginary part of the Lindhard function has the form shown in figure 5.4 (left panel). It is linear at low energy and corresponds to an arc of parabola at higher energy,

$$\chi_{nn}^{0''}(\mathbf{q}, \omega) = \begin{cases} \frac{\pi N(0)}{v_F |\mathbf{q}|} \omega & \text{for } 0 \leq \omega \leq |\omega_-(\mathbf{q})|, \\ \frac{\pi N(0)}{2\tilde{q}} \left[1 - \left(\tilde{\omega} - \frac{\tilde{q}}{2} \right)^2 \right] & \text{for } |\omega_-(\mathbf{q})| \leq \omega \leq \omega_+(\mathbf{q}), \end{cases} \quad (5.44)$$

where

$$\omega_{\pm}(\mathbf{q}) = \pm v_F |\mathbf{q}| + \frac{\mathbf{q}^2}{2m}. \quad (5.45)$$

The negative energy part can be deduced from (5.44) by noting that $\chi_{nn}^{0''}(\mathbf{q}, \omega) = -\chi_{nn}^{0''}(\mathbf{q}, -\omega)$.

For $\tilde{q} \geq 2$, the linear part is not present any more and the Lindhard function reduces to the arc of parabola (Fig. 5.4, right panel),

$$\chi_{nn}^{0''}(\mathbf{q}, \omega) = \frac{\pi N(0)}{2\tilde{q}} \left[1 - \left(\tilde{\omega} - \frac{\tilde{q}}{2} \right)^2 \right] \quad \text{for } \omega_-(\mathbf{q}) \leq \omega \leq \omega_+(\mathbf{q}). \quad (5.46)$$

Particle-hole pair excitation continuum

In the non-interacting system, the particle-hole pair excitation spectrum is defined by $\chi_{nn}^{0''}(\mathbf{q}, \omega) \neq 0$. It gives the values of (\mathbf{q}, ω) for which the equation $\omega = \epsilon_{\mathbf{k}+\mathbf{q}} - \epsilon_{\mathbf{k}}$ possesses at least a solution with $\xi_{\mathbf{k}} < 0$ and $\xi_{\mathbf{k}+\mathbf{q}} > 0$. For $|\mathbf{q}| \leq 2k_F$, the particle-hole continuum extends from $\omega = 0$ up to $\omega = \omega_+(\mathbf{q})$. For $|\mathbf{q}| > 2k_F$, there is no excitation at low energy and the particle-hole continuum extends from $\omega_-(\mathbf{q})$ to $\omega_+(\mathbf{q})$ (Fig. 5.5).

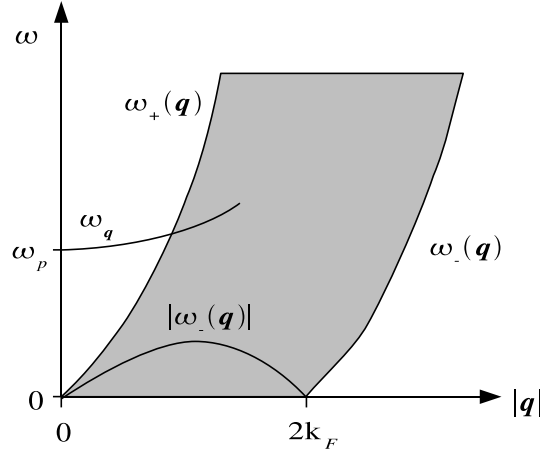


Figure 5.5: Plasmon mode dispersion $\omega_{\mathbf{q}}$ in the electron liquid. The shaded area shows the particle-hole excitation continuum. In the RPA the latter has the same boundaries as that of the non-interacting electron gas.

5.3.2 Density fluctuation spectrum

The spectrum of the density fluctuations can be obtained from the spectral function $\chi''_{nn}(\mathbf{q}, \omega) = \Im[\chi_{nn}^R(\mathbf{q}, \omega)]$ or the structure factor $S_{nn}(\mathbf{q}, \omega; T = 0) = 2\Theta(\omega)\chi''_{nn}(\mathbf{q}, \omega)$.⁸ In the RPA, there are two contributions to

$$S_{nn}^{\text{RPA}}(\mathbf{q}, \omega) = 2\Theta(\omega) \frac{\chi_{nn}^{0''}(\mathbf{q}, \omega)}{(1 + v(\mathbf{q})\Re[\chi_{nn}^{0R}(\mathbf{q}, \omega)])^2 + (v(\mathbf{q})\chi_{nn}^{0''}(\mathbf{q}, \omega))^2}. \quad (5.47)$$

The first one is due to a non-vanishing $\chi_{nn}^{0''}(\mathbf{q}, \omega)$ and comes from the particle-hole pair excitations. These are quite similar to the particle-hole pair excitations of the non-interacting electron gas and gives a continuous excitation spectrum (Fig. 5.5). The second contribution to the structure factor comes from the (collective) plasmon mode at the frequency $\omega_{\mathbf{q}}$ defined by

$$1 + v(\mathbf{q})\Re[\chi_{nn}^{0R}(\mathbf{q}, \omega_{\mathbf{q}})] = 0. \quad (5.48)$$

Such an excitation is well defined if its life-time – determined by $1/\chi_{nn}^{0''}(\mathbf{q}, \omega)$ – is long enough; only in this case does it show up as a sharp peak in $S_{nn}(\mathbf{q}, \omega)$ (Fig. 5.6). In the RPA, the plasmon has an infinite life-time as long as $\chi_{nn}^{0''}(\mathbf{q}, \omega) = 0$, i.e. as long as it does not overlap with the particle-hole pair continuum. When its energy satisfies $\omega = \epsilon_{\mathbf{k}+\mathbf{q}} - \epsilon_{\mathbf{k}}$ (with $|\mathbf{k}| < k_F$ and $|\mathbf{k}+\mathbf{q}| > k_F$), the plasmon becomes strongly damped (Landau damping) and is not a well-defined excitation of the system anymore. The absence of damping at small \mathbf{q} is an artifact of the RPA. Multipair excitations – not taken into account in the RPA – provides the main damping mechanism when Landau damping is ineffective. These issues have been discussed in detail in connection with the zero-sound mode of the neutral Fermi liquid (Secs. 4.3.3 and 4.3.5).

⁸The following discussion is similar to that of section 4.3.4 on the structure factor of the neutral Fermi liquid.

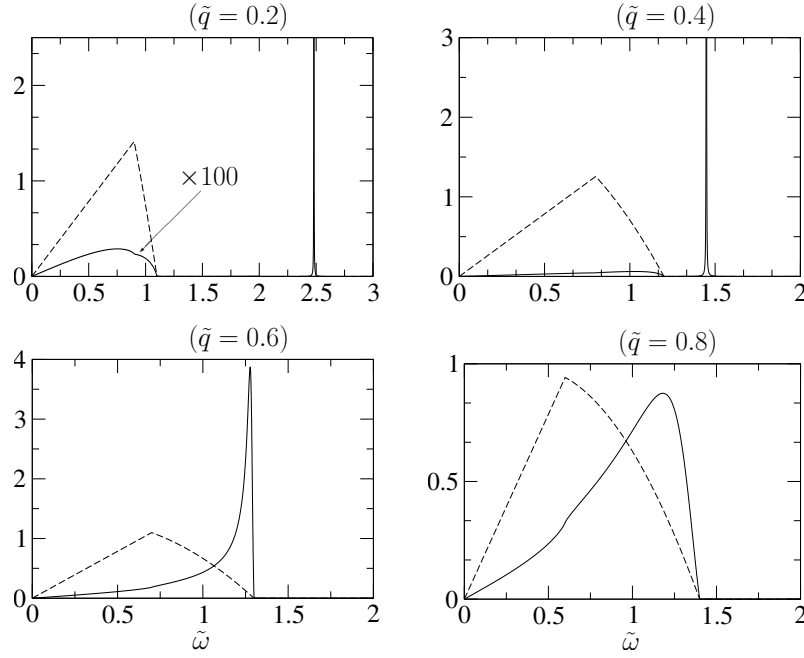


Figure 5.6: Structure factor $S_{nm}(\mathbf{q}, \omega)/4N(0)$ of the electron liquid in the RPA for different values of $\tilde{q} = |\mathbf{q}|/k_F$ and $r_s = 1$ ($\tilde{\omega} = \omega/v_F|\mathbf{q}|$). The dashed line shows the results for the non-interacting electron gas. The plots are obtained with a small but finite value of η (hence the nonzero width of the plasmon peak). For small values of \tilde{q} the plasmon peak is clearly visible – and gives the main contribution to the spectral weight $\int_0^\infty d\omega S_{nn}(\mathbf{q}, \omega)$ – while for larger values it merges with the continuum of particle-hole pair excitations.

Plasmon mode and sum rules

For $\mathbf{q} \rightarrow 0$ with ω fixed, $\chi_{nn}^{0R}(\mathbf{q}, \omega) \rightarrow -n\mathbf{q}^2/\omega^2m$, i.e.

$$\lim_{\mathbf{q} \rightarrow 0} \epsilon_{\parallel}^R(\mathbf{q}, \omega) = 1 - \frac{\omega_p^2}{\omega^2}, \quad (5.49)$$

and we recover $\omega_p = (ne^2/\epsilon_0m)^{1/2}$ as the excitation energy of the plasmon mode in the long-wavelength limit. Pushing the expansion of $\chi_{nn}^{0R}(\mathbf{q}, \omega)$ to higher order in \mathbf{q}^2 yields the long-wavelength plasmon dispersion

$$\omega_{\mathbf{q}}^2 = \omega_p^2 + \frac{3}{5}v_F^2\mathbf{q}^2 + \mathcal{O}(|\mathbf{q}|^4). \quad (5.50)$$

For $\mathbf{q} \rightarrow 0$ and $\omega \simeq \omega_p$, one has

$$\begin{aligned} 1 + v(\mathbf{q})\chi_{nn}^{0R}(\mathbf{q}, \omega) &\simeq (\omega + i\eta - \omega_p)v(\mathbf{q})\partial_\omega\chi_{nn}^{0R}(\mathbf{q}, \omega)\Big|_{\omega=\omega_p} \\ &= (\omega + i\eta - \omega_p)\frac{2}{\omega_p}, \end{aligned} \quad (5.51)$$

and therefore

$$\begin{aligned}\lim_{\mathbf{q} \rightarrow 0} \chi_{nn}^R(\mathbf{q}, \omega) &= -\frac{\omega_p}{2v(\mathbf{q})} \frac{1}{\omega + i\eta - \omega_p}, \\ \lim_{\mathbf{q} \rightarrow 0} \frac{1}{\epsilon_{\parallel}^R(\mathbf{q}, \omega)} &= 1 + \frac{\omega_p}{2} \frac{1}{\omega + i\eta - \omega_p}.\end{aligned}\tag{5.52}$$

Making use of (5.52), one obtains

$$\begin{aligned}\lim_{\mathbf{q} \rightarrow 0} \int_{-\infty}^{\infty} \frac{d\omega}{\pi} \omega \Im \left[\frac{1}{\epsilon_{\parallel}^R(\mathbf{q}, \omega)} \right]_{\text{plasmon}} &= -\omega_p^2, \\ \lim_{\mathbf{q} \rightarrow 0} \int_{-\infty}^{\infty} \frac{d\omega}{\pi} \frac{1}{\omega} \Im \left[\frac{1}{\epsilon_{\parallel}^R(\mathbf{q}, \omega)} \right]_{\text{plasmon}} &= -1.\end{aligned}\tag{5.53}$$

We conclude that the RPA satisfies the f -sum rule and the perfect-screening sum rule in the $\mathbf{q} \rightarrow 0$ limit, the plasmon mode exhausting the spectral weight. Equations (5.53) are exact. They are a consequence of the vanishing contribution of particle-hole pair excitations to the spectral function $\Im[1/\epsilon_{\parallel}^R(\mathbf{q}, \omega)]$ when $\mathbf{q} \rightarrow 0$.⁹

With $\epsilon_{\parallel}^R(\mathbf{q}, \omega) = 1 + v(\mathbf{q})\chi_{nn}^{0R}(\mathbf{q}, \omega)$, the longitudinal conductivity sum rule reduces to the f -sum rule for non-interacting electrons and is therefore trivially satisfied. The compressibility sum rule implies that the compressibility of the system equals that of the free electron gas. This agrees with the definition of the compressibility in a charged system, $n^2\kappa = \lim_{\mathbf{q} \rightarrow 0} \Pi_{nn}^R(\mathbf{q}, 0)$ (Sec. 3.4.1), since $\Pi_{nn} = \chi_{nn}^0$ in the RPA. If however, as in section 5.3.4 below, we compute the compressibility from the density dependence of the ground state energy the compressibility sum rule is violated.

5.3.3 Screening

Thomas-Fermi theory

Let us start with a simple theory of screening. We consider the response of an electron gas to a static impurity charge density $n_i(\mathbf{r})$. If the induced charge density varies slowly with respect to k_F , we expect a semiclassical description to be justified. The scalar potential $\phi(\mathbf{r})$ satisfies Poisson equation¹⁰

$$\nabla^2 \phi(\mathbf{r}) + \frac{e^2}{\epsilon_0} [\delta n(\mathbf{r}) + n_i(\mathbf{r})] = 0,\tag{5.54}$$

where $\delta n(\mathbf{r}) = \langle \hat{n}(\mathbf{r}) \rangle - n$ is the induced charge density. In a semiclassical picture, $\mu - \phi(\mathbf{r})$ acts as a local chemical potential and

$$\delta n(\mathbf{r}) = -\phi(\mathbf{r}) \frac{\partial n}{\partial \mu} + \mathcal{O}(\phi^2) = -n^2 \kappa \phi(\mathbf{r}) + \mathcal{O}(\phi^2),\tag{5.55}$$

where $\kappa = n^{-2} \partial n / \partial \mu = 3/2n\epsilon_F$ is the compressibility of the free electron gas. To first order in $\phi(\mathbf{r})$, Poisson equation then gives

$$\nabla^2 \phi(\mathbf{r}) - \frac{e^2}{\epsilon_0} n^2 \kappa \phi(\mathbf{r}) = -\frac{e^2}{\epsilon_0} n_i(\mathbf{r}).\tag{5.56}$$

⁹In Sec. 3.4.1, we have shown that the exact result $\lim_{\mathbf{q} \rightarrow 0} \omega_{\mathbf{q}} = \omega_p = (ne^2/\epsilon_0 m)^{1/2}$ can be deduced from the sum rules (5.53).

¹⁰See footnote 4 page 345.

In Fourier space, we find

$$\phi(\mathbf{q}) = \frac{e^2}{\epsilon_0} \frac{n_i(\mathbf{q})}{\mathbf{q}^2 + q_{\text{TF}}^2}, \quad (5.57)$$

where

$$q_{\text{TF}}^2 = \frac{e^2}{\epsilon_0} n^2 \kappa = \frac{3e^2 n}{2\epsilon_0 \epsilon_F} = r_s k_F^2 \frac{4}{\pi} \left(\frac{4}{9\pi} \right)^{1/3} \quad (5.58)$$

is the (square of the) Thomas-Fermi screening wave vector. From the standard definition of the longitudinal dielectric function,

$$\phi(\mathbf{q}) = \frac{e^2 n_i(\mathbf{q})}{\epsilon_0 \epsilon_{\parallel}(\mathbf{q}) \mathbf{q}^2}, \quad (5.59)$$

we obtain

$$\epsilon_{\text{TF}}(\mathbf{q}) = 1 + \frac{q_{\text{TF}}^2}{\mathbf{q}^2}. \quad (5.60)$$

At small distances ($|\mathbf{q}| \gg q_{\text{TF}}$), the impurity charge is unscreened since $\epsilon_{\text{TF}}(\mathbf{q}) \simeq 1$. On the contrary, at large distances the screening is very effective. For a point-like impurity $n_i(\mathbf{r}) = n_i \delta(\mathbf{r})$, the screened potential has the form of a Yukawa potential,

$$\phi(\mathbf{r}) = \frac{n_i e^2}{4\pi \epsilon_0 |\mathbf{r}|} \exp(-q_{\text{TF}} |\mathbf{r}|), \quad (5.61)$$

and is exponentially suppressed at length scales larger than the screening length q_{TF}^{-1} . Away from the impurity ($\mathbf{r} \neq 0$), the induced charge density is given by

$$\delta n(\mathbf{r}) = -\frac{\epsilon_0}{e^2} \nabla^2 \phi(\mathbf{r}) = -n_i q_{\text{TF}}^2 \frac{\exp(-q_{\text{TF}} |\mathbf{r}|)}{4\pi |\mathbf{r}|}. \quad (5.62)$$

A necessary condition for the (semiclassical) Thomas-Fermi theory to be justified is $q_{\text{TF}} \ll k_F$, i.e. $r_s \ll 1$. We shall see below that even when this condition is satisfied, the Thomas-Fermi theory fails to provide an accurate description of the response of the electron liquid to a static impurity charge density.

Static RPA dielectric function

In the RPA, the screening of a static impurity charge is determined by the dielectric function

$$\epsilon_{\text{RPA}}(\mathbf{q}) = 1 + \frac{q_{\text{TF}}^2}{2\mathbf{q}^2} \left\{ 1 - \frac{1}{\tilde{q}} \left(1 - \frac{\tilde{q}^2}{4} \right) \ln \left| \frac{\tilde{q} - 2}{\tilde{q} + 2} \right| \right\}. \quad (5.63)$$

For $\mathbf{q} \rightarrow 0$, one can approximate $\epsilon_{\text{RPA}}(\mathbf{q})$ by

$$\lim_{\mathbf{q} \rightarrow 0} \epsilon_{\text{RPA}}(\mathbf{q}) \simeq 1 + v(\mathbf{q}) \chi_{nn}^0(\mathbf{q} = 0) = \epsilon_{\text{TF}}(\mathbf{q}). \quad (5.64)$$

It is quite tempting to conclude that at long distances the RPA predicts results similar to those of the Thomas-Fermi theory. This turns out to be wrong because of the non-analyticity of $\epsilon_{\text{RPA}}(\mathbf{q})$ at $|\mathbf{q}| = 2k_F$. This non-analyticity, which originates in the Fermi surface of the electron gas, prevents the mere replacement $\epsilon_{\text{RPA}}(\mathbf{q}) \rightarrow$

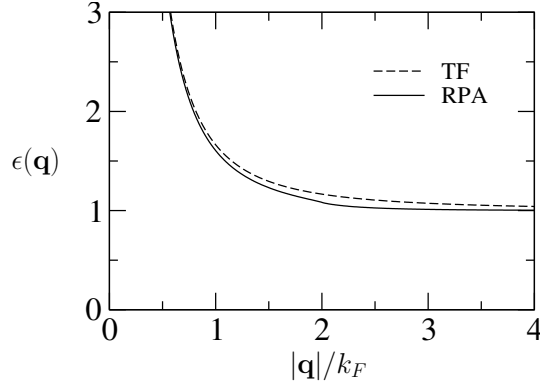


Figure 5.7: Static dielectric functions obtained from the Thomas-Fermi theory and the RPA. The non-analyticity of $\epsilon_{\text{RPA}}(\mathbf{q})$ at $|\mathbf{q}| = 2k_F$ gives rise to Friedel oscillations and a power-law decrease of the charge induced by a point-like impurity [Eq. (5.65)].

$\epsilon_{\text{TF}}(\mathbf{q})$ when computing the long-distance screening of an external potential. A careful analysis shows that the charge induced by a point-like impurity decays as a power law and exhibits Friedel oscillations [3],

$$\delta n(\mathbf{r}) \propto n_i \frac{\cos(2k_F |\mathbf{r}|)}{|\mathbf{r}|^3}, \quad (5.65)$$

in marked contrast with the results of the Thomas-Fermi theory [Eq. (5.62)].

5.3.4 Ground state energy and compressibility

Ground state energy

The thermodynamic potential can be expressed as a function of the interaction energy by means of a coupling constant integration. Let us write the Hamiltonian as $\hat{H} = \hat{H}_0 + \lambda \hat{H}_{\text{int}}$. We then have¹¹

$$Z = \text{Tr} e^{-\beta(\hat{H}_0 + \lambda \hat{H}_{\text{int}})}, \quad \frac{\partial \Omega}{\partial \lambda} = \frac{1}{\lambda} \langle \lambda \hat{H}_{\text{int}} \rangle_\lambda, \quad (5.66)$$

where the average $\langle \dots \rangle_\lambda$ is taken with the Hamiltonian $\hat{H}_0 + \lambda \hat{H}_{\text{int}}$. The potential energy can be expressed as a function of the density-density response function,

$$\begin{aligned} \langle \hat{H}_{\text{int}} \rangle_\lambda &= \frac{1}{2} \sum_{\mathbf{q}} v(\mathbf{q}) \left\langle \hat{n}(-\mathbf{q}) \hat{n}(\mathbf{q}) - \frac{\hat{N}}{V} \right\rangle_\lambda \\ &= \frac{1}{2} \sum_{\mathbf{q}} v(\mathbf{q}) \left[\frac{1}{\beta} \sum_{\omega_\nu} \chi_{nn}^\lambda(\mathbf{q}) e^{i\omega_\nu \eta} - n^\lambda \right], \end{aligned} \quad (5.67)$$

¹¹Note that \hat{H}_0 and \hat{H}_{int} do not commute in general. To compute $\partial Z / \partial \lambda$, one should expand $\text{Tr} e^{-\beta(\hat{H}_0 + \lambda \hat{H}_{\text{int}})}$, take the derivative with respect to λ , and use the cyclic invariance of the trace.

where both $\chi_{nn}^\lambda(q)$ and $n^\lambda = \langle \hat{N} \rangle_\lambda / V$ depend on λ . From (5.66) and (5.67), we obtain

$$\Omega = \Omega_0 + \int_0^1 \frac{d\lambda}{\lambda} \frac{1}{2} \sum_{\mathbf{q}} \lambda v(\mathbf{q}) \left[\frac{1}{\beta} \sum_{\omega_\nu} \chi_{nn}^\lambda(q) e^{i\omega_\nu \eta} - n^\lambda \right], \quad (5.68)$$

where $\Omega_0 \equiv \Omega(\lambda = 0)$ is the thermodynamic potential of the non-interacting electron gas.

In the RPA, one has

$$\chi_{nn}^\lambda(q) = \frac{\chi_{nn}^0(q)}{1 + \lambda v(\mathbf{q}) \chi_{nn}^0(q)} = \chi_{nn}^0(q) - \lambda v(\mathbf{q}) \frac{[\chi_{nn}^0(q)]^2}{1 + \lambda v(\mathbf{q}) \chi_{nn}^0(q)}. \quad (5.69)$$

Inserting (5.69) into (5.68) and summing over λ , one obtains the ground state energy

$$\begin{aligned} E_{\text{RPA}} &= \Omega(T=0) + \mu N = E_0 + E_x + E_{\text{corr}}^{\text{RPA}}, \\ E_x &= \frac{1}{2} \sum_{\mathbf{q}} v(\mathbf{q}) \left[\frac{1}{\beta} \sum_{\omega_\nu} \chi_{nn}^0(q) e^{i\omega_\nu \eta} - n \right], \\ E_{\text{corr}}^{\text{RPA}} &= \frac{1}{2\beta} \sum_{\mathbf{q}} \left\{ -v(\mathbf{q}) \chi_{nn}^0(q) + \ln [1 + v(\mathbf{q}) \chi_{nn}^0(q)] \right\}, \end{aligned} \quad (5.70)$$

with $\beta \rightarrow \infty$.

The kinetic energy per electron is given by

$$\frac{E_0}{N} = \frac{3}{5} \epsilon_F = \frac{3}{5} \left(\frac{9\pi}{4} \right)^{2/3} \frac{1}{r_s^2} \text{Ry}, \quad (5.71)$$

where the Rydberg $\text{Ry} = \frac{e^2}{8\pi\epsilon_0 a_0}$. An elementary calculation gives

$$E_x = -\frac{1}{V} \sum_{\mathbf{k}, \mathbf{q}} v(\mathbf{q}) n_{\mathbf{k}+\mathbf{q}}^0 (n_{\mathbf{k}}^0 - 1) - \frac{1}{2} \sum_{\mathbf{q}} v(\mathbf{q}) n = -\frac{1}{V} \sum_{\mathbf{k}, \mathbf{q}} v(\mathbf{q}) n_{\mathbf{k}+\mathbf{q}}^0 n_{\mathbf{k}}^0, \quad (5.72)$$

where $n_{\mathbf{k}}^0 = \Theta(k_F - |\mathbf{k}|)$. E_x is called the exchange energy. It is nothing but the first-order correction $\langle \hat{H}_{\text{int}} \rangle$ to the energy E_0 of the non-interacting electron gas and arises from the antisymmetry of the ground state with respect to the exchange of two particles (Fig. 5.8a).¹² The exchange energy per electron reads

$$\begin{aligned} \frac{E_x}{N} &= -\frac{1}{n} \int \frac{d^3 q}{(2\pi)^3} \int \frac{d^3 k}{(2\pi)^3} \frac{e^2}{\epsilon_0 |\mathbf{q} - \mathbf{k}|^2} \Theta(k_F - |\mathbf{k}|) \Theta(k_F - |\mathbf{q}|) \\ &= -\frac{e^2 k_F}{2\pi^2 \epsilon_0 n} \int \frac{d^3 k}{(2\pi)^3} \Theta(k_F - |\mathbf{k}|) \left[\frac{1}{2} + \frac{1 - \tilde{k}^2}{4\tilde{k}} \ln \left| \frac{1 + \tilde{k}}{1 - \tilde{k}} \right| \right] \\ &= -\frac{3e^2 k_F}{16\pi^2 \epsilon_0} \\ &= -\frac{3}{2\pi} \left(\frac{9\pi}{4} \right)^{1/3} \frac{1}{r_s} \text{Ry}. \end{aligned} \quad (5.73)$$

¹²The direct term involves $v(0)$ and vanishes in the jellium model.

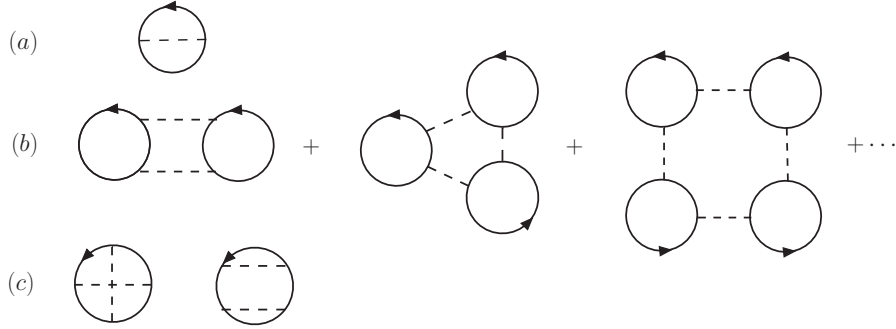


Figure 5.8: Feynman diagrams for the ground state energy $E = \Omega(T = 0) + \mu N$. (a) Exchange energy E_x . (b) Correlation energy $E_{\text{corr}}^{\text{RPA}}$ in the RPA. (c) Second-order contributions not included in $E_{\text{corr}}^{\text{RPA}}$.

The difference $E - E_0 - E_x$ is referred to as the correlation energy. In the RPA, it is given by (5.70) and corresponds to the bubble (or ring) diagrams shown in figure 5.8b. As the full calculation is not possible analytically, we only quote the final result [3],

$$\frac{E_{\text{corr}}^{\text{RPA}}}{N} = \frac{2}{\pi^2} (1 - \ln 2) \ln r_s - 0.141 \text{ Ry} \simeq 0.0622 \ln r_s - 0.141 \text{ Ry}. \quad (5.74)$$

The validity of the RPA can be improved by adding the second-order contributions shown in figure 5.8c. One then obtains the following expansion of the correlation energy in the high-density limit [3],

$$\frac{E_{\text{corr}}}{N} = 0.0622 \ln r_s - 0.094 + \mathcal{O}(r_s \ln r_s) \text{ Ry}. \quad (5.75)$$

Compressibility

Let us introduce the notation $E/N = \epsilon(r_s)$ with

$$\epsilon(r_s) = \frac{3}{5} \left(\frac{9\pi}{4} \right)^{2/3} \frac{1}{r_s^2} - \frac{3}{2\pi} \left(\frac{9\pi}{4} \right)^{1/3} \frac{1}{r_s} + 0.0622 \ln r_s - 0.094 + \mathcal{O}(r_s \ln r_s) \text{ Ry}. \quad (5.76)$$

We then obtain the pressure

$$P = - \left. \frac{\partial E}{\partial V} \right|_N = n^2 \frac{\partial \epsilon}{\partial n} = - \frac{nr_s}{3} \frac{\partial \epsilon}{\partial r_s} \quad (5.77)$$

and the inverse compressibility

$$\frac{1}{\kappa} = -V \left. \frac{\partial P}{\partial V} \right|_N = n \frac{\partial P}{\partial n} = \frac{nr_s}{3} \left[-\frac{2}{3} \frac{\partial \epsilon}{\partial r_s} + \frac{r_s}{3} \frac{\partial^2 \epsilon}{\partial r_s^2} \right]. \quad (5.78)$$

The compressibility becomes negative for $r_s > 4.84$ (Fig. 5.9). As noted in section 3.4.1, the condition $\kappa < 0$ does not necessarily imply an instability of the system as κ does not include the stiffness of the background of positive charge with respect to a change of volume.¹³

¹³ κ [Eq. (5.78)] is calculated by assuming that the background of positive charge adjusts itself to maintain neutrality at not energy cost (Sec. 3.4.1).

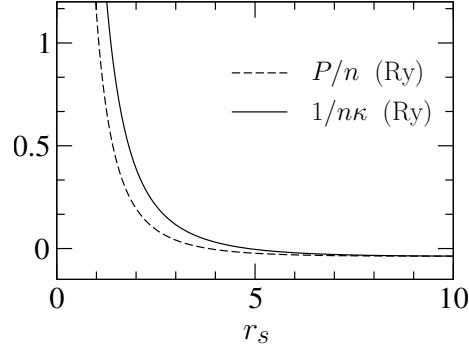


Figure 5.9: Pressure P and compressibility κ of the electron liquid obtained from (5.76).

5.4 One-particle properties

So far we have computed the collective excitations of the electron liquid assuming that the one-electron properties are similar to that of the non-interacting electron gas. This assumption is qualitatively correct if the electron liquid is a Fermi liquid (in the sense discussed in chapter 4). If it were not the case, self-energy corrections in the one-particle propagator would invalidate our calculation of the density-density response function. In this section we show that the electron liquid is indeed a Fermi liquid.

5.4.1 Hartree-Fock theory

When discussing the RPA in the functional integral formalism, we obtained the Hartree self-energy at the saddle-point (or mean-field) approximation. The Hartree self-energy vanishes in the jellium model because of the neutrality of the system. A natural improvement over the Hartree theory amounts to including the exchange (or Fock) term shown in figure 5.10,

$$\begin{aligned}
 \Sigma_x(\mathbf{k}) &= -\frac{1}{\beta V} \sum_{\mathbf{k}'} v(\mathbf{k}' - \mathbf{k}) G(\mathbf{k}') e^{i\omega'_n \eta} \\
 &= -\frac{1}{\beta V} \sum_{\mathbf{k}'} v(\mathbf{k}' - \mathbf{k}) \frac{e^{i\omega'_n \eta}}{i\omega'_n - \xi_{\mathbf{k}'} - \Sigma_x(\mathbf{k}')} \\
 &= -\frac{1}{V} \sum_{\mathbf{k}'} v(\mathbf{k}' - \mathbf{k}) n_F[\xi_{\mathbf{k}'} + \Sigma_x(\mathbf{k}')]. \tag{5.79}
 \end{aligned}$$

Note that Σ_x is independent of the frequency. At zero temperature one therefore obtains

$$\Sigma_x(\mathbf{k}) = -\frac{1}{V} \sum_{\mathbf{k}'} v(\mathbf{k}' - \mathbf{k}) \Theta(k_F - |\mathbf{k}'|), \tag{5.80}$$



Figure 5.10: Diagrammatic representation of the exchange (or Fock) self-energy Σ_x . The thick solid line denotes the Green function $G = (G_0^{-1} - \Sigma_x)^{-1}$.

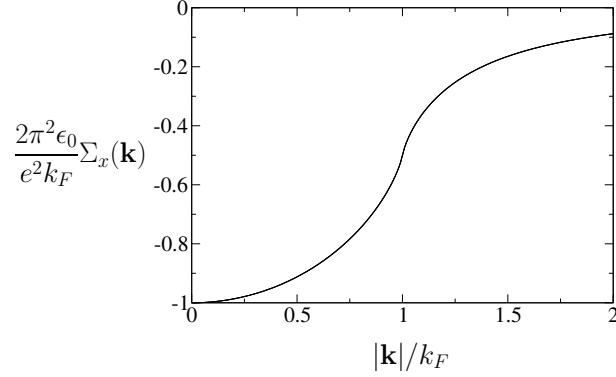


Figure 5.11: Exchange self-energy $\Sigma_x(\mathbf{k})$ vs. $\tilde{k} = |\mathbf{k}|/k_F$.

where the Fermi wave vector is defined by $\xi_{k_F} + \Sigma_x(k_F) = 0$ and

$$n = \frac{2}{\beta V} \sum_{\mathbf{k}} G(k) e^{i\omega_n \eta} = \frac{2}{V} \sum_{\mathbf{k}} n_F[\xi_{\mathbf{k}} + \Sigma_x(\mathbf{k})] = \frac{2}{V} \sum_{\mathbf{k}} \Theta(k_F - |\mathbf{k}|). \quad (5.81)$$

Thus k_F is the same as in the non-interacting electron gas. This is nothing but the Luttinger theorem: the interactions do not change the volume of the Fermi surface (Sec. 4.4.6). For a frequency independent self-energy, the theorem is trivially satisfied. From (5.80), we thus obtain

$$\Sigma_x(\mathbf{k}) = -\frac{e^2 k_F}{2\pi^2 \epsilon_0} \left[\frac{1}{2} + \frac{1 - \tilde{k}^2}{4\tilde{k}} \ln \left| \frac{1 + \tilde{k}}{1 - \tilde{k}} \right| \right] \quad (5.82)$$

(Fig. 5.11), where $\tilde{k} = |\mathbf{k}|/k_F$.

Since

$$\frac{\Sigma_x(k_F)}{\epsilon_F} = -\frac{e^2 m}{2\pi^2 \epsilon_0 k_F} = -\frac{2}{\pi k_F a_0} \sim -r_s, \quad (5.83)$$

the exchange self-energy is small in the high-density limit $r_s \ll 1$ where a perturbative treatment of the Coulomb interaction is expected to be valid. Yet the Hartree-Fock theory is unphysical for the electron liquid. The reason is that the non-analyticity of $\Sigma_x(\mathbf{k})$ at $|\mathbf{k}| = k_F$ gives rise to a vanishing effective mass at the Fermi level,

$$\frac{m}{m^*} = 1 + \frac{m}{k_F} \frac{\partial}{\partial |\mathbf{k}|} \Sigma_x(\mathbf{k}) \Big|_{k_F} = \lim_{\tilde{k} \rightarrow 1} \left[1 + \frac{1}{\pi k_F a_0} \ln \left| \frac{2}{1 - \tilde{k}} \right| \right] = \infty. \quad (5.84)$$

5.4.2 RPA self-energy

To understand the failure of the Hartree-Fock theory in the electron liquid we relate the self-energy to the density-density response function using the general formula

$$\frac{1}{\beta V} \sum_k \Sigma(k) G(k) e^{i\omega_n \eta} = \frac{1}{2V} \sum_{\mathbf{q}} v(\mathbf{q}) \left[\frac{1}{\beta} \sum_{\omega_\nu} \chi_{nn}(q) e^{i\omega_\nu \eta} - n \right]. \quad (5.85)$$

One easily deduces from (5.85) that the Hartree-Fock approximation ($\Sigma = \Sigma_x$) corresponds to the density-density response function

$$\tilde{\chi}_{nn}^0(q) = -\frac{2}{\beta V} \sum_k G(k) G(k+q), \quad (5.86)$$

obtained from the non-interacting susceptibility χ_{nn}^0 by replacing the bare propagator G_0 by $G = (G_0^{-1} - \Sigma_x)^{-1}$. $\tilde{\chi}_{nn}^0$ does not include screening and is a very poor approximation to the density-density response function of the electron liquid. Since the RPA does include screening and gives a rather satisfying account of density fluctuations (Sec. 5.3), a much better approximation for the self-energy is

$$\Sigma(k) = -\frac{1}{\beta V} \sum_q \frac{v(\mathbf{q})}{1 + v(\mathbf{q}) \tilde{\chi}_{nn}^0(q)} G(k+q). \quad (5.87)$$

The corresponding expression for the density-density response function has the RPA form with all one-particle propagators dressed with the self-energy (5.87). Whether or not this is an improvement over the RPA will be discussed in section 5.5. In this section we focus on the self-energy (5.87). In order to simplify its computation, we give up self-consistency and replace G by G_0 . The resulting expression,

$$\begin{aligned} \Sigma_{\text{RPA}}(k) &= -\frac{1}{\beta V} \sum_q \frac{v(\mathbf{q})}{1 + v(\mathbf{q}) \chi_{nn}^0(q)} G_0(k+q) \\ &= -\frac{1}{\beta V} \sum_q \frac{v(\mathbf{q})}{\epsilon_{\parallel}^{\text{RPA}}(q)} G_0(k+q) \end{aligned} \quad (5.88)$$

is referred to as the RPA self-energy. It is similar to the exchange self-energy with the Coulomb interaction $v(\mathbf{q})$ replaced by the effective interaction $v(\mathbf{q})/\epsilon_{\parallel}^{\text{RPA}}(q)$ and without the self-consistency. The RPA self-energy can be rewritten as

$$\Sigma_{\text{RPA}}(k) = -\frac{1}{\beta V} \sum_q v(\mathbf{q}) G_0(k+q) + \frac{1}{\beta V} \sum_q v(\mathbf{q})^2 \chi_{nn}^{\text{RPA}}(q) G_0(k+q), \quad (5.89)$$

as shown in figure 5.12.

Fermi-liquid results

In order to show that the RPA self-energy describes a Fermi liquid, one must verify that the imaginary part $\Im[\Sigma_{\text{RPA}}^R(\mathbf{k}, \omega)]$ varies as $\omega^2 + \pi^2 T^2$ at low energies and temperatures (Sec. 4.4). The first term in the rhs of (5.89), Σ_x , does not contribute to

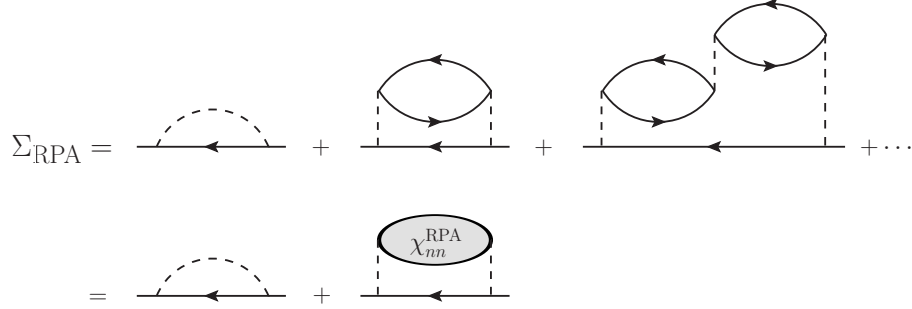


Figure 5.12: Diagrammatic representation of the RPA self-energy.

$\Im[\Sigma_{\text{RPA}}^R(\mathbf{k}, \omega)]$. The second term is similar to the second-order contribution to the self-energy studied in section 4.4.1 with the bare charge susceptibility χ_{nn}^0 replaced by χ_{nn}^{RPA} . We therefore deduce from (4.168)

$$\begin{aligned} \Im[\Sigma_{\text{RPA}}^R(\mathbf{k}, \omega)] &= -\frac{m}{4\pi^2 k_F} \int_0^{2k_F} v(\mathbf{q})^2 |\mathbf{q}| d|\mathbf{q}| \\ &\quad \times \int_{-\infty}^{\infty} d\omega' \chi_{nn}^{\text{RPA}''}(\mathbf{q}, \omega') [n_B(\omega') + n_F(\omega' + \omega)]. \end{aligned} \quad (5.90)$$

Because of the Bose and Fermi factors, the relevant part of the sum over ω' corresponds to $|\omega'| \leq \max(|\omega|, T)$. For $|\omega|, T \rightarrow 0$, we can therefore use the low-energy limit of $\chi_{nn}^{\text{RPA}''}(\mathbf{q}, \omega')$ (with $|\mathbf{q}| \leq 2k_F$),

$$\begin{aligned} \lim_{\omega \rightarrow 0} \chi_{nn}^{\text{RPA}''}(\mathbf{q}, \omega) &= \lim_{\omega \rightarrow 0} \frac{\chi_{nn}^{0''}(\mathbf{q}, \omega)}{(1 + v(\mathbf{q}) \Re[\chi_{nn}^{0R}(\mathbf{q}, \omega)])^2 + (v(\mathbf{q}) \chi_{nn}^{0''}(\mathbf{q}, \omega))^2} \\ &= \lim_{\omega \rightarrow 0} \frac{\chi_{nn}^{0''}(\mathbf{q}, \omega)}{[1 + v(\mathbf{q}) \chi_{nn}^{0R}(\mathbf{q}, 0)]^2} \\ &= \frac{\pi N(0) \omega}{[\epsilon_{\parallel}^{\text{RPA}}(\mathbf{q}, 0)]^2 v_F |\mathbf{q}|}. \end{aligned} \quad (5.91)$$

Since $\chi_{nn}^{\text{RPA}''}(\mathbf{q}, \omega)$ is linear in ω for $\omega \rightarrow 0$, we can proceed as in section 4.4.1 to obtain

$$\Im[\Sigma_{\text{RPA}}^R(\mathbf{k}, \omega)] = -\frac{m^3}{16\pi^3 k_F} \int_0^{2k_F} d|\mathbf{q}| \frac{v(\mathbf{q})^2}{[\epsilon_{\parallel}^{\text{RPA}}(\mathbf{q}, 0)]^2} (\omega^2 + \pi^2 T^2), \quad (5.92)$$

which is the standard Fermi-liquid result. Approximating $\epsilon_{\parallel}^{\text{RPA}}(\mathbf{q}, 0)$ by the Thomas-Fermi result $\epsilon_{\text{TF}}(\mathbf{q}) = 1 + q_{\text{TF}}^2/q^2$, we find

$$\int_0^{2k_F} d|\mathbf{q}| \frac{v(\mathbf{q})^2}{[\epsilon_{\parallel}^{\text{RPA}}(\mathbf{q}, 0)]^2} = \frac{2\pi^4}{m^2 k_F} \xi(r_s), \quad (5.93)$$

where

$$\xi(r_s) = \int_0^1 dx \left[1 + \frac{\pi}{r_s} \left(\frac{9\pi}{4} \right)^{1/3} x^2 \right]^{-2}. \quad (5.94)$$

r_s	0	1	2	3	4	5	6
$z_{k_F}^{\text{RPA}}$	1	0.859	0.768	0.700	0.646	0.602	0.566
$(m^*/m)_{\text{RPA}}$	1	0.97	0.99	1.02	1.04	1.06	1.08

Table 5.2: Quasi-particle weight z_{k_F} [6] and effective mass m^* (reproduced from [1]) in the RPA.

We deduce that the quasi-particle life-time is given by

$$\frac{1}{\tau_{\mathbf{k}}} = -2z_{\mathbf{k}}\Im[\Sigma^R(\mathbf{k}, \tilde{\xi}_{\mathbf{k}})] = z_{\mathbf{k}}\frac{\pi}{8}\xi(r_s)\frac{\tilde{\xi}_{\mathbf{k}}^2 + \pi^2T^2}{\epsilon_F}, \quad (5.95)$$

where $z_{\mathbf{k}}$ is the quasi-particle weight and $\tilde{\xi}_{\mathbf{k}}$ the quasi-particle dispersion defined by $\tilde{\xi}_{\mathbf{k}} = \xi_{\mathbf{k}} + \Re[\Sigma^R(\mathbf{k}, \tilde{\xi}_{\mathbf{k}})]$ (Sec. 4.4). In the high-density limit $r_s \rightarrow 0$, $\xi(r_s) \sim \sqrt{r_s}$ and (5.95) gives

$$\frac{1}{\tau_{\mathbf{k}}} \sim z_{\mathbf{k}}\sqrt{r_s}\frac{\tilde{\xi}_{\mathbf{k}}^2}{\epsilon_F} \sim z_{\mathbf{k}}\omega_p\frac{\tilde{\xi}_{\mathbf{k}}^2}{\epsilon_F^2} \quad (5.96)$$

($T = 0$). The quasi-particle scattering rate is proportional to the plasma frequency but reduced by the factor $\tilde{\xi}_{\mathbf{k}}^2/\epsilon_F^2$. At metallic densities $r_s \sim 1$, $\xi(r_s) \sim 1$ and $1/\tau_{\mathbf{k}} \sim z_{\mathbf{k}}\tilde{\xi}_{\mathbf{k}}^2/\epsilon_F$.

We have argued in section 4.4.1 that the ω^2 dependence of the self-energy is expected to be a sufficient condition for the quasi-particle weight $z_{\mathbf{k}}$ to be finite on the Fermi surface. The calculation of $z_{\mathbf{k}}$ – as well as the effective mass m^* – is quite cumbersome and we therefore only quote the results in table 5.2. As expected, z_{k_F} decreases monotonically with r_s but remains finite, confirming the Fermi-liquid behavior of the electron liquid up to rather large values of r_s . The effective mass is smaller than the bare mass when $r_s \lesssim 2$, but becomes larger at sufficiently low density.¹⁴

5.5 Beyond the RPA

On the one hand, the RPA appears to provide a satisfying approximation of a metal in many respects. Not only does it account for important physical properties (plasmon mode, screening, etc.), but it also satisfies a number of exact results such as the sum rules discussed in sections 5.2.1 and 5.3.2 or the value of the plasmon energy in the long wavelength limit. On the other hand it is essentially a mean-field approximation as the correlations between a given electron and the other particles are not taken into account. For instance,

- the Pauli principle – that follows from the antisymmetry of the N -electron wave function – reduces the probability of finding two electrons with the same spin orientation nearby. This “exchange hole” is not accounted for in the RPA.

¹⁴This suggests that the Landau parameter F_1^s is negative in the high-density limit of the three-dimensional electron liquid ($m^*/m = 1 + F_1^s/3$ in a Galilean invariant system (Sec. 4.1.3)). This agrees with predictions of local field factor approaches (Sec. 5.5) [1].

- the probability of finding two electrons nearby, irrespective of their spin orientations, is further altered by the Coulomb interaction. This “correlation hole” is also absent in the RPA.

To take into account the exchange and correlation holes, one has to go beyond the RPA. The difficulty is to set up an approximation that does not spoil the nice aspects of the RPA such as the agreement with exact results (e.g. the fulfillment of sum rules).

Difficulties of diagrammatic expansions

The difficulty to set up diagrammatic approximations that satisfy exact results such as sum rules or conservation laws (that follow from symmetries) is a very important issue. To understand this point, let us consider the following property

$$\chi_{nn}(\mathbf{q} = 0, i\omega_\nu \neq 0) = 0, \quad (5.97)$$

which is a consequence of particle conservation.¹⁵ In the RPA, (5.97) is satisfied since $\chi_{nn}^0(\mathbf{q} = 0, i\omega_\nu \neq 0) = 0$. Consider now the density-density response function

$$\tilde{\chi}_{nn}(q) = \frac{\tilde{\chi}_{nn}^0(q)}{1 + v(\mathbf{q})\tilde{\chi}_{nn}^0(q)} \quad (5.98)$$

obtained from χ^{RPA} by replacing the bare propagator G_0 by the dressed propagator $G = (G_0^{-1} - \Sigma)^{-1}$ [Eq. (5.86)]. The precise form of Σ does not matter for our discussion. Using the spectral representation ??? of $G(k)$, we obtain

$$\tilde{\chi}_{nn}^0(q) = -\frac{2}{V} \sum_{\mathbf{k}} \int_{-\infty}^{\infty} d\omega' d\omega'' A(\mathbf{k}, \omega') A(\mathbf{k} + \mathbf{q}, \omega'') \frac{n_F(\omega') - n_F(\omega'')}{i\omega_\nu + \omega' - \omega''}, \quad (5.99)$$

where $A(\mathbf{k}, \omega) = -\frac{1}{\pi} \Im[G^R(\mathbf{k}, \omega)]$. For $\mathbf{q} = 0$, (5.99) can be written as

$$\begin{aligned} \tilde{\chi}_{nn}^0(\mathbf{q} = 0, i\omega_\nu) &= \frac{2}{V} \sum_{\mathbf{k}} \int_{-\infty}^{\infty} d\omega' d\omega'' A(\mathbf{k}, \omega') A(\mathbf{k}, \omega'') \\ &\quad \times [n_F(\omega') - n_F(\omega'')] \frac{\omega'' - \omega'}{\omega_\nu^2 + (\omega' - \omega'')^2}. \end{aligned} \quad (5.100)$$

For free electrons, $A(\mathbf{k}, \omega) = \delta(\omega - \xi_{\mathbf{k}})$ and $\chi_{nn}^0(\mathbf{q} = 0, i\omega_\nu \neq 0) = 0$. For interacting electrons, $A(\mathbf{k}, \omega)$ is not a delta peak and values of ω', ω'' such that $\omega' \neq \omega''$ will contribute in (5.100). Since $[n_F(\omega') - n_F(\omega'')](\omega'' - \omega') \geq 0$, $\tilde{\chi}_{nn}^0(\mathbf{q} = 0, i\omega_\nu \neq 0)$ cannot vanish and particle conservation is violated. The only way to restore particle conservation is to include “vertex” corrections in the calculation of the irreducible part Π_{nn} of the density-density response function χ_{nn} . Vertex corrections cannot be taken into account by a mere renormalization of the one-particle propagator but rather correspond to a renormalization of the interaction vertex $v(\mathbf{q})$. Diagrammatically, they are represented by Coulomb lines joining the particle and hole lines in Π_{nn} .¹⁶

¹⁵Particle conservation implies that $\hat{n}(\mathbf{q} = 0) = \hat{N}/\sqrt{V}$ commutes that the Hamiltonian. It follows that $\hat{n}(\mathbf{q} = 0, \tau) = e^{\tau\hat{H}}\hat{n}(\mathbf{q} = 0)e^{-\tau\hat{H}} = \hat{n}(\mathbf{q} = 0)$ and $\chi_{nn}(\mathbf{q} = 0, \tau) = \text{const}$; hence (5.97).

¹⁶The second diagram in Fig 5.1 corresponds to a vertex correction, the following ones to self-energy corrections.

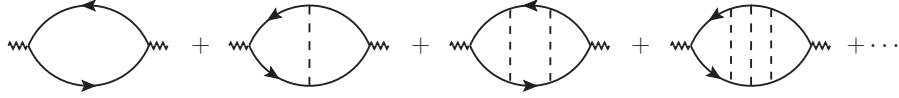


Figure 5.13: Π_{nn} in the time-dependent Hartree-Fock approximation. The one-particle propagator includes the exchange self-energy Σ_x .

The simplest approximation beyond the RPA includes both the Hartree and the Fock self-energies in the one-particle propagator; it is sometimes referred to as the time-dependent Hartree-Fock approximation (the RPA corresponding to the time-dependent Hartree approximation). In order to satisfy conservation laws and other exact results, one must then include all ladder diagrams in the calculation of Π_{nn} (Fig. 5.13). The justification of this statement will be given in chapter 9 where a general method – based on the Luttinger-Ward functional – to generate diagrammatic approximations that satisfy conservation laws will be given. The time-dependent Hartree-Fock approximation requires a numerical solution. It does not yield a significant improvement over the RPA and furthermore has its own limitations and difficulties. A detailed discussion of the results is beyond the scope of this chapter; we refer the interested reader to Ref. [1].

Local field factors

It is possible to treat exchange and correlation effects in a non-diagrammatic approximation that preserves the mathematical structure of the RPA. In the latter, the electrons are subjected to an effective potential

$$\phi_{\text{ext}}(\mathbf{q}, \omega) + v(\mathbf{q})\langle \hat{n}(\mathbf{q}) \rangle(\omega) \quad (5.101)$$

(Sec. 5.2.2). In order to account for the correlations neglected in the RPA, one assumes that the effective potential seen by the spin- σ electrons can be written as

$$\begin{aligned} \phi_{\text{eff},\sigma}(\mathbf{q}, \omega) &= \phi_{\text{ext}}(\mathbf{q}, \omega) + v(\mathbf{q}) \sum_{\sigma'} \langle \hat{n}_{\sigma'}(\mathbf{q}) \rangle(\omega) \\ &\quad - \sum_{\sigma'} v(\mathbf{q}) G_{\sigma\sigma'}(\mathbf{q}, \omega) \langle \hat{n}_{\sigma'}(\mathbf{q}) \rangle(\omega). \end{aligned} \quad (5.102)$$

The local field factor $G_{\sigma\sigma'}(\mathbf{q}, \omega)$ contains the correction to the effective potential stemming from the exchange and correlation effects. The density-density response function then reads [1]

$$\chi_{nn}(q) = \frac{\chi_{nn}^0(q)}{1 + v(\mathbf{q})[1 - G_+(q)]\chi_{nn}^0(q)}, \quad (5.103)$$

where $G_+(q) = \frac{1}{2}[G_{\uparrow\uparrow}(q) + G_{\uparrow\downarrow}(q)]$. Thus the local field factor can be seen as an effective vertex correction. The local field factor approach has proven to be a successful method to calculate many quantities of interest (effective mass, compressibility, spin susceptibility, Landau parameters, etc.) while treating exchange and correlation effects beyond the RPA. Again we refer to Ref. [1] for a detailed discussion.

Guide to the bibliography

The electron liquid is discussed in Refs. [1–5] where many references to original works can be found. An excellent and remarkably complete discussion of the subject is given in Ref. [1].

Bibliography

- [1] G. F. Giuliani and G. Vignale, *Quantum Theory of the Electron Liquid* (Cambridge University Press, 2005).
- [2] G. D. Mahan, *Many-particle physics*, 2nd edition, chapter 5 (Plenum press, New York, 1990).
- [3] A. L. Fetter and J. D. Walecka, *Quantum Theory of Many-Particle Systems* (Dover, 2003).
- [4] D. Pines and P. Nozières, *The Theory of Quantum Liquids* (Addison-Wesley, 1968).
- [5] A.-M. Tremblay, *Le problème à N corps*, chapter 5 (unpublished).
- [6] L. Hedin, Phys. Rev. **139**, A796 (1965).